

Experimental Simulation of Runback Ice

Rajnish K. Calay,* Arne E. Holdø,† and Philip Mayman‡
University of Hertfordshire, Hatfield AL10 9AB, England, United Kingdom

and
Isaac Lun§
City University of Hong Kong, Kowloon, Hong Kong

A series of wind-tunnel tests on a NACA 0012 airfoil was conducted to simulate the aerodynamic effects of runback ice. The drag and lift effects on the airfoil were assessed using wind-tunnel balance for three geometries of triangular section ice shapes at three different chordal positions. The results show a great degree of sensitivity of the aerodynamic flow characteristics to the shape and the chordal position of the ice accretion, and thereby highlight the need for realistic prediction models for runback ice.

Introduction

THE formation of ice on aircraft wings and control surfaces has been a subject of great concern. Large amounts of information are available on the formation of ice, its accretion, and aerodynamics effects.^{1–3} Most studies have focused on the prediction of ice accretion on wings to design better ice-protection systems and to ensure their efficient performance. Ice-protection systems should allow controlled formation of ice that creates no adverse aerodynamic effects. Two methods are adopted for preventing ice formation: 1) de-icing and 2) anti-icing. De-icing is where ice accretion is permitted on the protected surface and then removed periodically. Anti-icing is where moisture is prevented from freezing on the protected surfaces.

Anti-icing comes in two forms: 1) running dry and 2) running wet. Running dry is where all of the moisture impinging on the surface is evaporated with no runback. Running wet anti-icing system prevents ice formation on the leading edge by heating of airfoils. Because of this, another ice-related phenomenon develops that is caused by the water from the melted ice on the leading edge being driven over the cold, nonheated part of the airfoil. This water eventually turns into ice at some distance downstream of the leading edge, it is termed runback ice, and is the subject of this paper. Direct impingement of water on these unprotected parts also contributes to runback ice formation by varying amounts that is increasing closer to the leading edge. This having happened, runback ice is not subject to removal by a de-icing system. Thus, it must be shown in the certification of an aircraft that safe performance will remain, despite the expected formation of runback ice.

Currently, research in running wet anti-icing systems is limited and runback ice is treated in a basic level. Few prediction models for runback water have been reported recently.^{4,5} However, experimental work is needed to achieve a better understanding of the behavior of runback water and the formation of runback ice.

The modeling of the complete physical process is very expensive if it is to be carried out for all conditions. Methods for modeling the effect of runback ice have therefore been

developed. One method consists of using a small object resembling the ice front positioned at various chordwise locations on the upper surface of the wing. While this method does not simulate the dynamic effects of runback ice, it models the aerodynamic effects caused by the geometric distortions of the airfoil shape because of the runback ice.

The aim of the present work was to investigate the aerodynamic effects of runback ice using wind-tunnel testing methods. The tests employed geometric representations of runback ice of varying relative size and shape located at differing chordwise positions to assess the aerodynamic effects.

Experimental Details

A NACA 0012 shape airfoil was used. This airfoil has a symmetrical geometry with a maximum thickness of 12% chord at the 30% chordal position.⁶ The chord length for the present model was 1 m. The test airfoil was placed and tested in the 1.15 × 0.84 m low-speed (30 m/s), closed-return, circuit-type wind tunnel at the University of Hertfordshire.

Three configurations of ice shapes, right-angled step-shape triangle (SS), flat-shape triangle (SF), and right-angled ramp-shape triangle (SR) were used (Fig. 1) to resemble the ice front. These geometries were tested at various chordal positions, 5, 15, and 25% chord lengths from the leading edge. The ice shapes were defined according to the procedure associated with the most critical ice shapes that may form while the ice protection system is operated normally.⁷

The right-angled triangle (with the vertical edge facing freestream) represented the ice that would form in a region where direct impingement of water onto the wing played a large part in ice formation. Such a region where the surface is exposed to the free surface is very close to the leading edge (approximately 1% chord). This situation represented the inner wing de-ice off configuration where a clear, narrow parting strip is maintained along the leading edge by the anti-ice system. It also represents residual ice resulting from direct impingement of large droplets beyond a pneumatic boot de-icing.³

The flat-shape triangle represents the ice that would form in a region where direct impingement of moisture onto a wing played a negligible part compared with the contribution from water running back over the wing surface. Thus, the flat-shape triangle appeared to more accurately represent the ice shape on the outboard wing with the anti-ice system protecting the upper surface back to at least 10% chord.

A third shape for runback ice simulation was defined to be the so-called ramp shape. This shape is also a right-angled triangle as shown in Fig. 1, but with the vertical face pointing in the lee direction. This shape arises from the argument that,

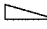
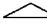
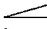
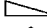
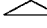


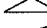
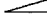
Received March 1, 1996; revision received Nov. 19, 1996; accepted for publication Nov. 20, 1996. Copyright © 1996 by the American Institute of Aeronautics and Astronautics, Inc. All rights reserved.

*Research Fellow, Fluid Dynamics, Mechanical/Aeronautical Engineering Division.

†Reader, Fluid Dynamics, Mechanical/Aeronautical Engineering Division.

‡Research Student, Mechanical/Aeronautical Engineering Division.

§Research Assistant, Building and Construction Engineering.

CONFIGURATION	SIMULATED ICE SHAPE	
	TYPE	POSITION
1		5%
2		5%
3		5%
4		15%
5		15%
6		15%
7		25%
8		25%
9		25%

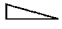

SIZE OF SIMULATED ICE SHAPE	
	Base - 14mm
	Height - 3.5mm

Fig. 1 Test configurations.

with negligible direct water impingement, the aerodynamic forces would cause the water running back over the surface to form an ice shape with a bias of ice buildup on the downstream edge. The project did not aim to prove any ice shape right or wrong, but to provide a comparison between the aerodynamic effects of the various shapes. Furthermore, the ice shapes are influenced by transient factors that were difficult to simulate within the scope of this investigation. The varying chordal positions for ice shapes represented the ice formation points corresponding to the range of performance of an ice protection system, i.e., from a very small amount of protection up to considerable protection.

The simulated ice shapes were machined to the designed shape geometry from a solid aluminum bar to produce adequate shape accuracy. The model was completely spanned by ice shapes and no gap existed at the joints between the ice shapes and the airfoil surface. The model was mounted on two forward struts and one rear strut. These struts were shielded from the airfoil by streamlined guards to prevent the effects of the wind on the struts. Lift, drag, and pitching moments were measured by the electromechanical balance situated below the working section of the wind tunnel.

Forty-one pressure tapings were used to record the measurements of pressure over the airfoil upper surface. A pitot-static tube was located upstream of the model and used to measure the freestream total pressure and static pressure head. Wake velocity profiles were measured by using a rake comprising 72 pitot tubes. Fifty pitot tubes with 3-mm spacing were clustered in the center position of the rake to provide detailed information of the wake profile. The 22 border tubes read freestream, i.e., undisturbed, manometer head values. This ensured that the disturbed airflow was captured by the middle 50 tubes. The rake was mounted 65-mm downstream of the airfoil. A second pitot static tube was placed to the left of the rake and used together with the first pitot static tube (upstream of the airfoil) to monitor freestream values.

Initial experiments were conducted for the clean airfoil to obtain the clean airfoil pressure distribution to do the following:

- 1) Validate equipment and data collection/processing techniques.
- 2) Compare the experimental data with theoretically calculated pressure distributions.
- 3) Analyze the two dimensionality of the flow over the model airfoil.

The contribution of drag arising from exposed lengths of the model struts was evaluated and the obtained drag values for the airfoil were corrected accordingly. The three-dimensional

effects that may exist over the ends of the model were eliminated by the use of sideplates. The corrections to account for the tunnel boundary were also applied to the measured data. Once sensible results and trends were established, further tests were conducted using different ice shapes. A full range of positive incidences from 0 deg to stall were used for each configuration. A single tunnel speed of 30 ms^{-1} (Reynolds number 1.25×10^6) was used for the tests. All configurations were tested with airfoil incidence angles of 0, 8, 14, 16, and 18 deg.

Results and Discussion

Effect of Ice Shapes on Airfoil Pressure Distribution

Figure 2 shows a comparison of pressure distributions between the clean airfoil and that obtained from testing the various ice shapes at a chordal position of 5% and an airfoil incidence of 0 deg. The basic effects on pressure distribution caused by ice shapes are obvious. These are 1) a high-pressure trough immediately in front of the ice shape and 2) a low-pressure peak immediately behind the ice shape. These observations can be explained by considering the flow behavior around the ice shape as shown in Fig. 3. It can be seen that just in front of the shape there is a region of strong recirculation. This slowing down of the air causes a high-pressure point just in front of the ice shape. The region of disturbance extends forward toward the leading edge. This is indicated by the increase in pressure immediately upstream of the ice shape, compared with the case for the clean airfoil where the flow continued to accelerate in this region, causing motion. The extent to which a flow can be influenced upstream of the ice shapes is more clearly seen in Fig. 4 for the ice shapes at the 25% chordal position. Here, the flow departs from clean airfoil distribution as far upstream as the 15% chord position.

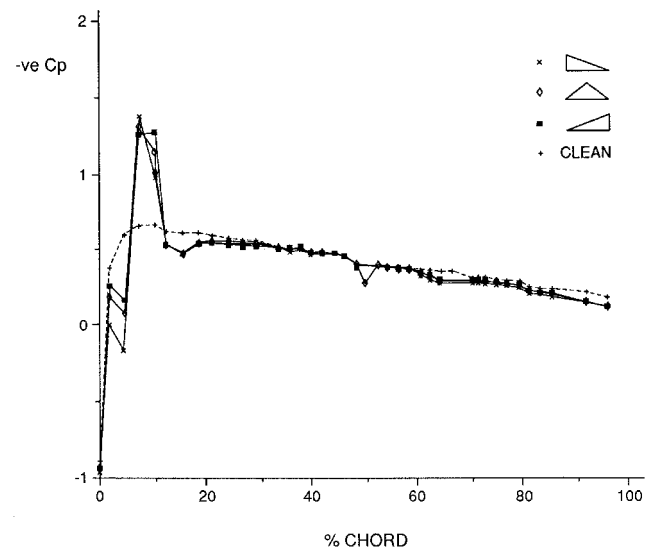


Fig. 2 Pressure distribution for clean airfoil and simulated ice front at 5% chordal position at airfoil incidence of 0 deg.

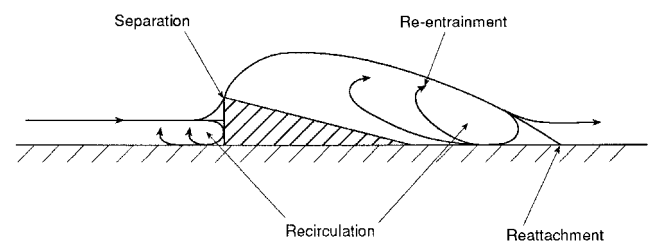


Fig. 3 Typical representation of flowfield around the ice shape.

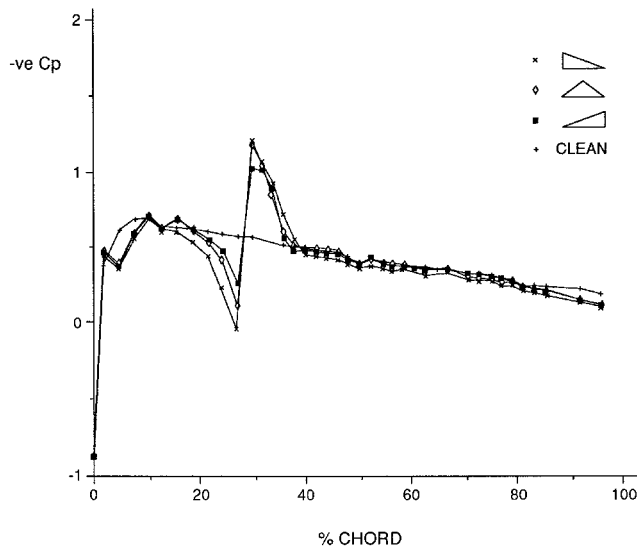


Fig. 4 Pressure distribution for different ice shapes at 25% chordal position.

The low-pressure peak immediately after the ice shape is caused by the region of separated flow, following separation at the top corner of the ice shape. The separation causes a low-pressure region followed by increasing pressure toward and a little beyond the point of reattachment.

Effects of Varying the Runback Ice Shapes

The difference between the pressure distribution caused by a different-shaped ice front is clear in Fig. 2. The variation in the high-pressure trough just upstream of the ice shapes is caused by the varying degree of recirculation. The step shape with its abrupt barrier to the airflow causes strong recirculation. With a change in the inclination of the windward side from 90 to 157 deg for the flat shape and from 90 to 168 deg for the ramp shape, the shapes become more streamlined. The effect of this is a reduction in disturbance to the flow, and hence, weaker recirculation with continued acceleration of the main flow up the forward-facing slope of shapes.

The discrepancies in the heights of the low-pressure peaks is believed to be a result of the varying degrees of disturbance inflicted on the airflow by the shapes. The separated wake from the step shape has stronger vortices than that from the flat shape which, in turn, is stronger than the ramp triangle. The higher local velocities thus created give the step triangle the highest suction peak, with the flat triangle and ramp triangle following in sequence.

The variation in sharpness of the suction peaks is because of the different positions of reattachment of the separated airflow. The ramp shape maintains the same low-pressure value for the first two tappings following the ice shape. This represents a distance of about six times the step height, and the actual reattachment length will be somewhere between the second and third tappings after the ice shape that is at a distance between 6–10 step heights (Fig. 1). This is in agreement with the findings of Kim⁸ that, for a backward-facing step, mean reattachment length is seven step heights.

The bluntness of the peak for the ramp shape contrasts with the shape peak for the step shape, with the flat shape forming a compromise. This suggests that the airflow reattaches further downstream for the ramp shape than for the flat shape that, in turn, reattaches downstream of that for the step shape. This, however, is mainly because of the varying positions of separation on the different shapes, i.e., the airflow separates at the upstream edge of the ramp triangle. Further flow visualization is necessary to investigate the effect on reattachment length of varying ice-shape geometry.

Effects of Varying Runback Ice Position

The effects of varying simulated ice position were shown in Fig. 5, where the pressure distributions for the ramp shape ice front at the varying test chordal position at 0-deg incidence are compared. Observations of the pressure peaks and troughs show that they reduce in magnitude, as the ice shape is moved farther downstream, but approximately the same shape and proportions relative to the ice shapes are maintained. This trend suggests that the effects of the shape on the airflow become less severe downstream. The reasons for this occurring are because as the ice shape is moved downstream, it is getting farther away from the critical leading-edge region, where the clean airfoil upper surface suction is at its greatest and airflow at its fastest.

Figure 6 shows the corresponding pressure distributions for the step shape at 0 deg. It shows a slight increase in magnitude of the pressure peak and trough from 5 to 15% chord, and then a subsequent reduction in magnitude for 25% chord. This may be because at 0-deg incidence, clean airfoil pressure coefficient C_p values are at their lowest magnitude, and the maximum pressure coefficient $C_{p_{max}}$ is actually away from the leading edge at a chordal position of 10%. The pressure dis-

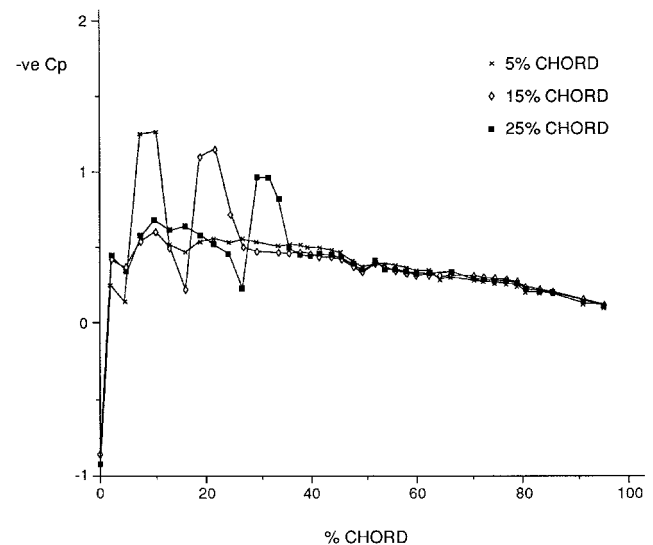


Fig. 5 Pressure distribution for ramp shape ice front at various chordal positions and 0-deg airfoil incidence.

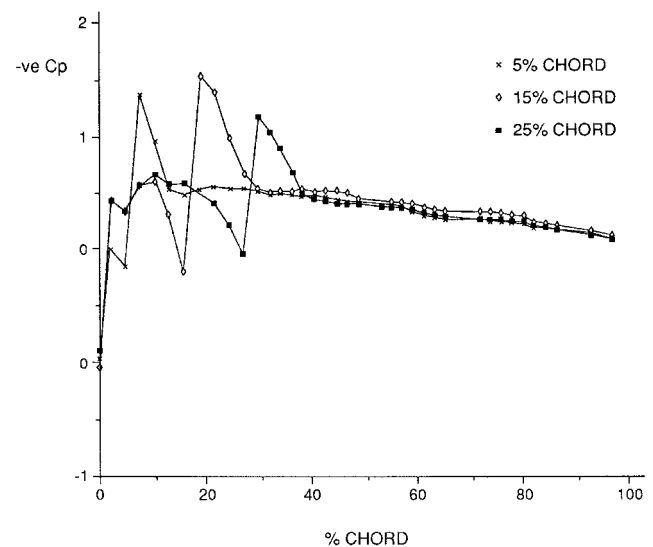


Fig. 6 Pressure distribution for step shape ice front at various chordal positions and 0-deg airfoil incidence.

tribution for 5% ice front at chord position shows a second pressure trough following a low-pressure peak (Fig. 2). This emphasizes the sensitivity to a flow disturbance of this region of the airfoil. However, the shape and position of this trough is the same for all three ice shapes at 5% chord, irrespective of the varying reattachment lengths for the different shapes.

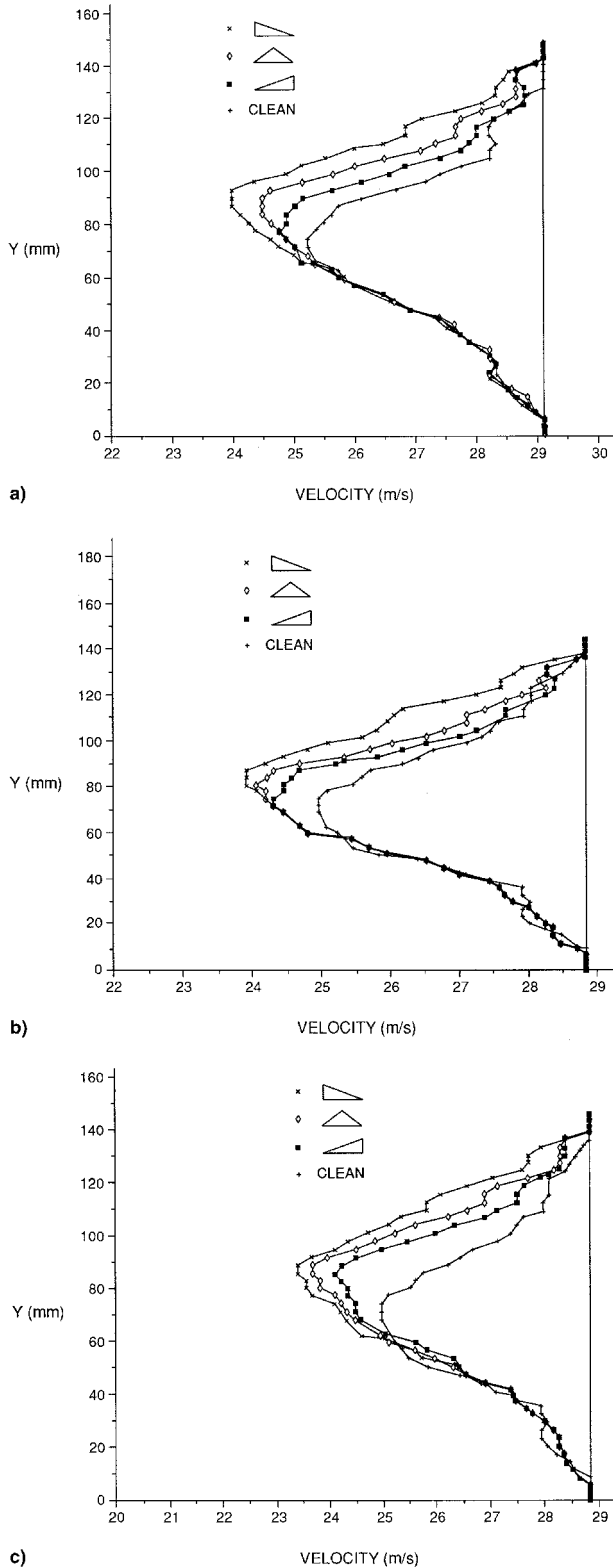


Fig. 7 Wake velocity profiles for different ice shapes at a) 5, b) 15, and c) 25% chordal position.

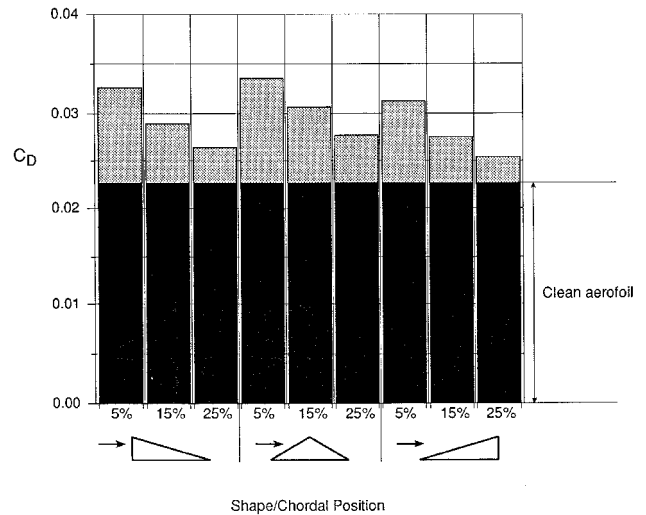


Fig. 8 Comparison of drag coefficient for various ice shapes at different chordal positions with the clean airfoil.

Effects on Airfoil Drag

The wake velocity profiles for various ice fronts at 5, 15, and 25% chordal positions, respectively, at 0-deg incidence are shown in Figs. 7a–7c. The effects of the ice shapes attached to the upper surface of the airfoil are restricted to the upper portion of the resulting wake, with the lower wake remaining the same. Two distinct effects, namely, increasing magnitude of velocity loss and vertical extent on the upper wake, are clearly displayed by the different shapes of simulated ice. The magnitude of velocity loss increases with increasing magnitude for ramp, flat, and step shape, respectively. This shows that the drag will increase in this sequence and with increments proportional to the increase of area under the curves on the velocity profiles as the sequence is traversed.

The effect on the drag of different geometry of the simulated ice is shown in Fig. 8 for the various chordal positions. At all chordal positions, the clean airfoil drag increase is increased by the presence of ice shapes. The variation in drag because of the change from a ramp shape to a flat shape is approximately the same as changing from a flat shape to a step shape. The effect on the drag because of ice formation at three chordal position can also be observed. The relative effect on drag as the chordal position is varied is similar for each of the three shapes.

Effects of Runback Ice on Lift

Figures 9a–9c show variation of lift coefficient C_L with respect to incident angle for different ice-front shapes at different chordal positions. The comparison of stall behavior of clean aerofoil with an aerofoil with ice front at different chordal positions can be clearly seen in Figs. 10a–10c. The lift curves for the three ice shapes positioned at 5% chord show initial stalling around an incidence of 12–14 deg (Fig. 10a). C_L values continue to increase, in an unpredictable fashion, for the remainder of incidence tested and do not achieve a conventional NACA 0012 type stall.

The behavior for the ice shapes at 5% chord is caused by the flow, separated by the ice shapes, alternately succeeding and failing to reattach to the airfoil at incidences above the initial stall point. Effectively, at these incidences, the reattachment length has become too long to be accommodated by the airfoil. This behavior continues past the normal NACA 0012 stall incidence of 16 deg because of the presence of ice shapes delaying total upper surface separation. The initial stall was observed during testing around 12 deg by the airfoil starting to shake.

Being farther away from the leading edge, the ice shapes at 15 and 25% chord positions do not have such a drastic effect on the lift curve as those at 5% chord. However, the initial

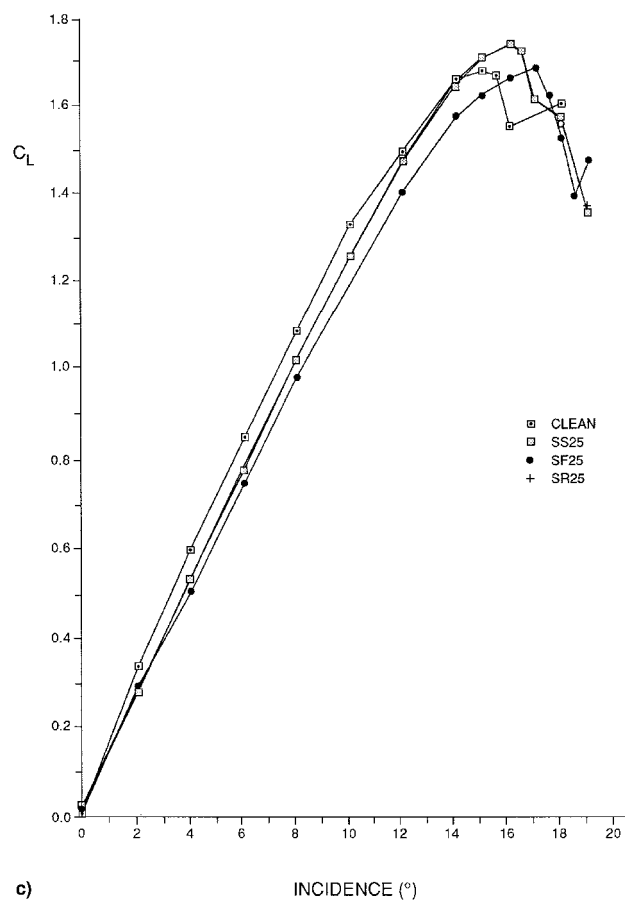
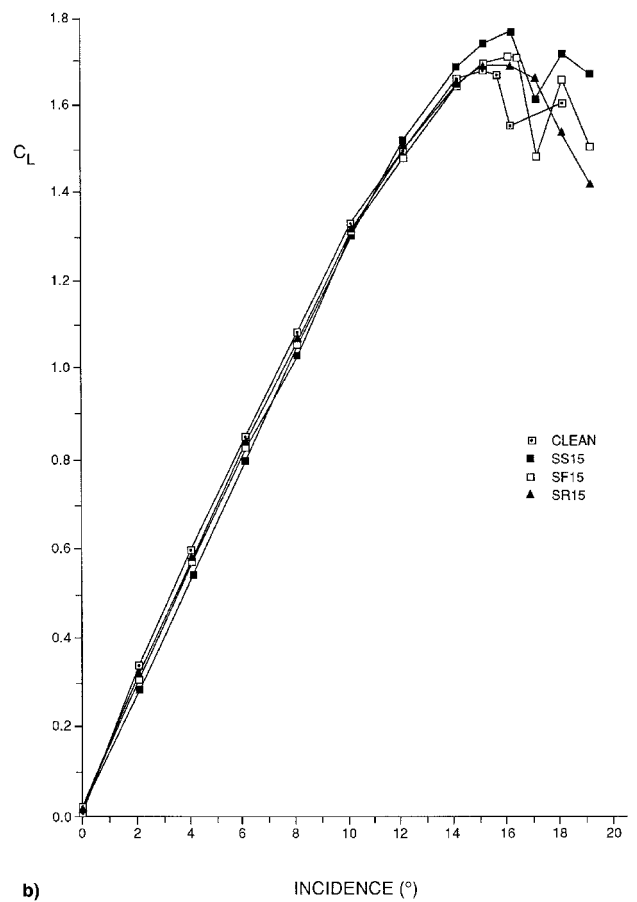
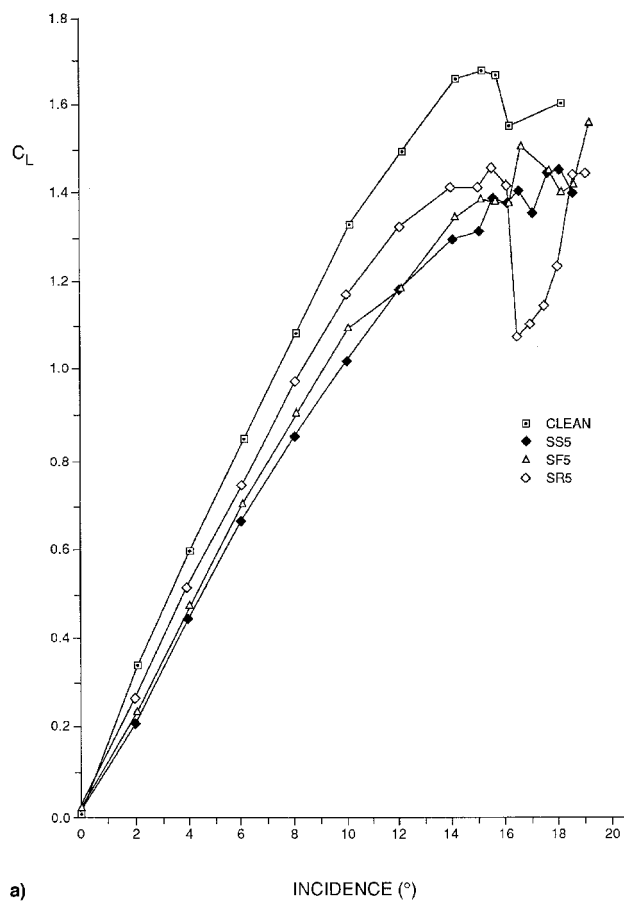


Fig. 9 Comparison of lift coefficient for various ice shapes at a) 5, b) 15, and c) 25% chord with the clean airfoil.

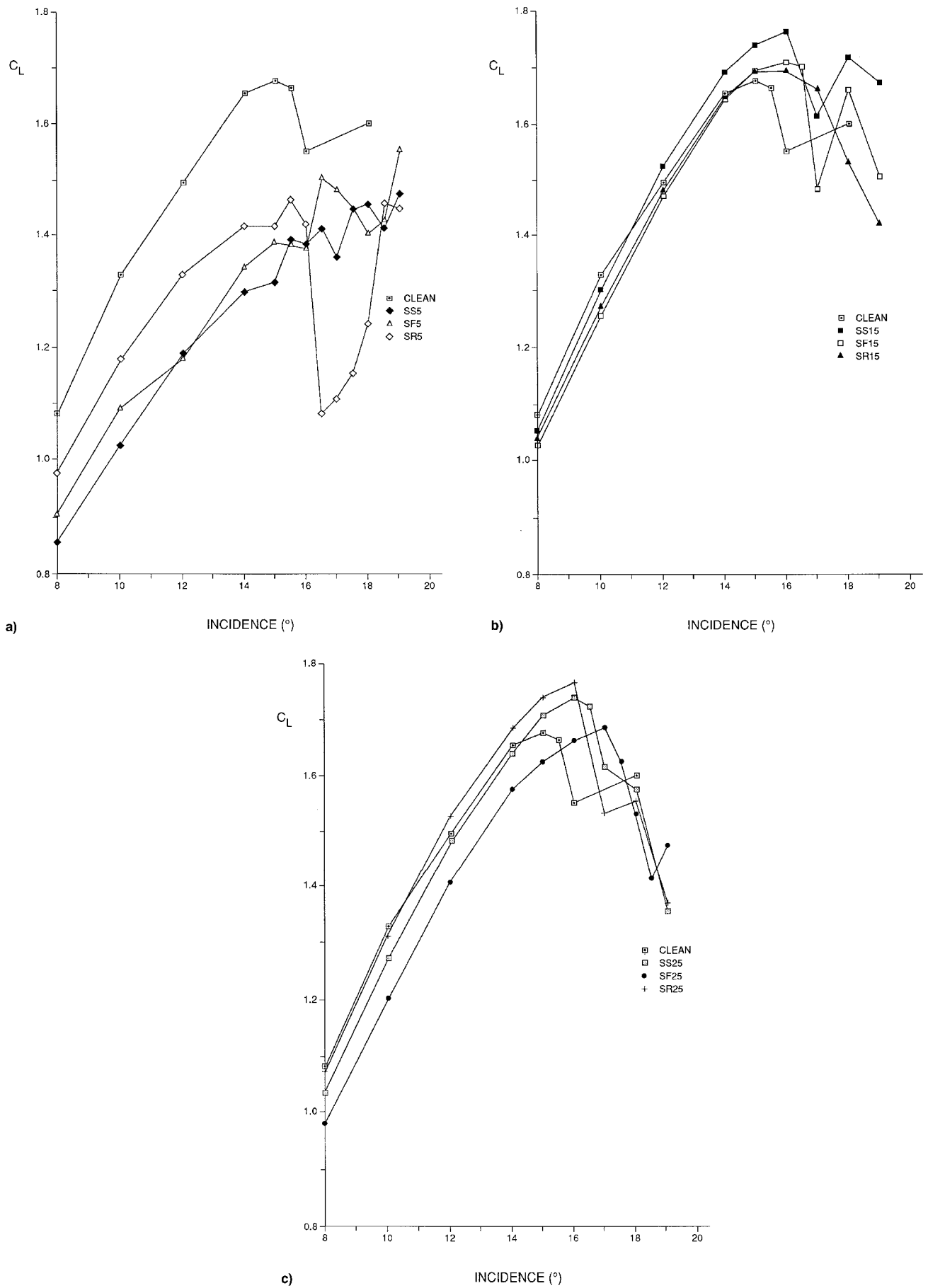


Fig. 10 Comparison of stall behavior for simulated ice configurations at a) 5, b) 15, and c) 25% chord.

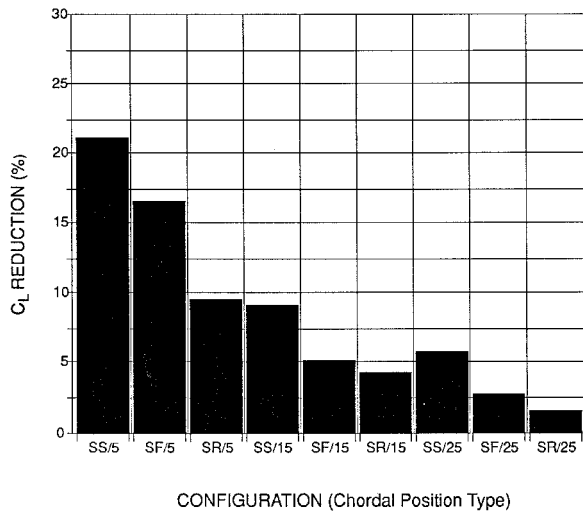


Fig. 11 Comparison of lift coefficient between various ice shapes at different chordal positions and at an incident angle of 8 deg.

flow visualization tests showed that the stalls of all simulated ice configurations are initiated from the ice shape, unlike the clean aerofoil stall that is of the trailing-edge type. It is also shown that $C_{L_{max}}$ is actually increased slightly by having the simulated ice shapes at 15 or 25% chord. This is because the lift curve for the clean airfoil begins to diverge from the initial straight line around 12 deg as a result of the separation beginning at the outer flow from the upper surface at the trailing edge. This led to a stall point in this test series of 15 deg. The ice-shape lift curves, however, show that the beginning of separation is delayed because of maintaining flow attachment against the positive pressure gradient. Thus, when stalling does occur around 16 deg, a higher $C_{L_{max}}$ has been attained.

The lift curve for the step-shape ice shape at 15% chord shows significantly lower values of C_L than the other shapes at this chordal position, but continues to $C_{L_{max}}$ at 17-deg incidence. This is because of the extra turbulence created by the shape that, although detrimental to the lift curve as a whole, delays the stall beyond that for the other configurations.

Figure 11 shows that lift loss increases with respect to ice shape for ramp, flat, and step shapes, respectively. The increase with respect to chordal attachment position is in ascending order for 25, 15, and 5%. It was observed that the relative effects of simulated ice position do not change with the incidences, as depicted in Fig. 11 for 8-deg incidence. This case illustrates the results for all cases and is at an incidence before the premature stalling of the 5% chord configurations were initiated.

The investigation has highlighted the need for predicting the runback ice shapes and simulating their effects carefully, so that the aircraft truly demonstrates its ability to maintain safe degrees of control and handling throughout and following an ice encounter. Though this may basically seem to be stating an obvious fact, the study has shown that apparently small changes in ice configuration can produce large changes in aerodynamic behavior. This means that slight inaccuracies in the prediction of runback ice may result in the simulation of aerodynamic behavior being unacceptable. The findings encourage development of the use of numerical methods for predicting the nature of runback ice formation. One way for studying runback ice as two-phase flow is by computational fluid dynamics. However, this requires resolving several numerical parameters to achieve accurate simulation.⁹ There are other factors such as the change in the ice shapes with respect to time and related aerodynamic flow characteristics that also need detailed consideration. More experimental data may be required to achieve database on the dynamic and aerodynamic behavior of runback ice.

Conclusions

The relative aerodynamic effects of simulated runback ice of three shapes at three chordal positions were investigated by wind-tunnel experimental methods. Lift loss and airfoil drag increase for ramp, flat, and step shapes representing runback ice at different chordal positions of 25, 15, and 5% were studied. The following flow characteristics were observed as a result of runback ice.

1) As the position of ice shape is moved backward from the 5% position, the lift loss associated with the step shape increases relative to that for the ramp shape. Conversely, the lift loss associated with the flat shape decreases relative to that for the ramp shape. For example, the step shape at 8-deg incidence and chordal position of 25% causes 3.8 times the ramp shape lift loss, compared with the flat shape that produces only 1.8 times the ramp shape lift loss.

2) For any particular shape, lift loss reduces more for a movement from 5 to 15% chord than for a similar movement from 15 to 25% chord. For example, at 8-deg incidence, the flat shape at 5% produces a lift loss 9.1 times that for the 15% position, compared with the 15% chord position that produces only 1.9 times the 25% position lift loss. The decrease in lift loss with backward movement of chordal position does not hold strictly true for comparison of various shapes. This is demonstrated, for example, by the step shape at 25% chord, producing greater lift losses than the flat and ramp shape at 15% chord.

3) At 5% chord position, the drag increase for the flat shape reduces with the increasing incidence relative to the drag increase for the ramp shape until two shapes have a similar drag increase. Whereas, the drag decrease for step shape continues to increase by typically 40% more than the ramp section.

4) Increase in incidence at the 5% chord position results in disproportionately large drag increase for all ice shapes when compared with drag increase at 15 and 25% chord positions. However, the reduction in drag with backward movement of ice shapes is not the same for all shapes. For example, at 8-deg incidence, the step shapes at 25% chord produce a greater C_D than the flat and ramp shapes at 15% chord.

5) The attachment of simulated runback ice to the airfoil changes the nature of the stall by causing separation to initiate from the ice shape rather than the trailing edge. Premature stall around 14-deg incidence occurs because of ice shape attached at 5% chordal position. Stall may be delayed and $C_{L_{max}}$ slightly increases by ice shapes at 15 and 25% chord positions.

References

- ¹Shaw, R. J., Potapczuk, M. G., and Bidwell, C. S., "Predictions of Airfoil Aerodynamic Performance Degradation Due to Ice," *Numerical and Physical Aspects of Aerodynamic Flows IV*, edited by T. Cebeci, Springer-Verlag, New York, 1990.
- ²Shin, J., Berkowitz, B., Chen, H. H., and Cebec, T., "Prediction of Ice Shapes and Their Effect on Airfoil Drag," *Journal of Aircraft*, Vol. 31, No. 2, 1994, pp. 263–270.
- ³Bragg, M. B., "Aircraft Aerodynamic Effects Due to Large Droplet Ice Accretions," AIAA Paper 96-0932, Jan. 1996.
- ⁴Al-Khalil, K. M., Keith, T. G., and De Witt, K. J., "Numerical Modelling of Runback Water on Ice Protected Aircraft Surfaces," 5th Symposium on Numerical and Physical Aspects of Aerodynamic Flows, Long Beach, CA, Jan. 1992.
- ⁵Al-Khalil, K. M., Keith, T. G., and De Witt, K. J., "Development of an Improved Model for Runback Water on Aircraft Surfaces," *Journal of Aircraft*, Vol. 31, No. 2, 1994, pp. 271–278.
- ⁶Abbot, I. H., and Doenhoff, E. V., *Theory of Wing Sections*, 2nd ed., Dover, New York, 1959.
- ⁷Mayman, P., "Runback Ice Simulation," BEng Project Rept., Univ. of Hertfordshire, Hatfield, England, UK, 1990.
- ⁸Kim, J. J., "Investigation of Separation and Reattachment of a Turbulent Shear Layer; Flow over a Backward Facing Step," Ph.D. Dissertation, Stanford Univ., Stanford, CA, 1978.
- ⁹Lun, I., Calay, R. K., and Holdø, A. E., "Modelling Two-Phase Flows Using CFD," *Applied Energy*, Vol. 53, No. 3, 1996, pp. 299–314.